Mechanical analysis of a drilling riser based on a pipe-in-pipe model

Huanhuan Wang[a], Jin Yang[a*], Svein Sævik[b], Bernt J Leira[b]

a College of Safety and Ocean Engineering, China University of Petroleum-Beijing, Beijing, 102249, China

b Department of Marine Technology, Norwegian University of Science and Technology, Trondheim, 7052, Norway

Abstract

Due to the presence of a drill string inside drilling risers, the mechanical analysis becomes somewhat challenging which has attracted attention from design engineers and drilling operators. The purpose of this study is to investigate the response of a riser with a drill string inside based on the FEM method, and to compare the numerical results with those corresponding to single pipe conditions. Two different riser models were studied, (i) Single Pipe Model: the riser system is assumed to consist of a single pipe, (ii) Pipe-in-Pipe (PIP) model: the riser system comprises an outer riser with an internal drill string. Both the single pipe and the PIP models were established within the framework of the global riser analysis software Riflex. Mechanical analysis of a deep-water riser in the South China Sea was performed in order to compare the riser response behavior obtained by application of the two different models. In the case of static analysis, modest differences were observed, whereas the dynamic analysis demonstrated more significant deviations between results based on the two models. The characteristics of the riser response for the PIP model were further investigated in terms of the displacements, dynamic motion and stress distribution. A definition of an influence coefficient in order to account for the effect of the drill string on the mechanical behavior of the riser was proposed, and the influence of the drill string corresponding to different top tension levels and environmental conditions was discussed.

Keywords：Drilling riser; Pipe-in-pipe condition; Dynamic analysis; Deep-water drilling

1. Introduction

A large number of oil fields in deep waters have been discovered and in general this requires further exploratory drilling for the purpose of resource mapping. However, deep-water drilling technology is very different from that applied for shallow waters. [1,2] In deep-water drilling projects, risers are the key device that connects the drilling platform to the subsea wellhead [3]. In addition to bottom tension and self-weight, the riser has to resist environmental loads as well as the internal drill string and loads caused by the drilling fluid. Riser safety during deep-water drilling is therefore challenging, which seriously affects the safety of such drilling operations [4]. Therefore, the research on riser mechanical behavior during deep-water drilling has become an increasingly important issue.

The riser is a key component which connects the drilling platform to the subsea wellhead. Its mechanical behavior is affected by the joint effect of marine environment and drilling conditions. Previously, a significant amount on research has been carried out in relation to the mechanical behavior of drilling risers. In 1966, Fischer and Ludwig [5] first discussed the design of shallow-water risers, revealing the importance of axial tension and bottom joints, formulation of static equilibrium equations and studying the role of dynamic loads from wave kinematics and floater motions. Burke [6] solved the static differential equation of the riser and analyzed the influence of top tension, lateral offset and current on the static performance. He was the first to formulate the riser dynamic equilibrium equations using D'Alembert's principle and the Morison equation to describe the wave and current loads. The dynamic performance of the riser was investigated accordingly.

Static analysis is the basis for assessing riser mechanical behavior. O'Brien et al. [7,8] have described their three-dimensional nonlinear motions formulation and applied this to practical analysis of flexible risers. The works of McNamara and O'Brien provide a structured approach to computation of the flexible riser static profile.[9] In 1988, Engseth et al. [10] developed a computer program for advanced analysis of flexible marine riser systems. The program is tailored for this application both with respect to system modelling and efficiency of solution strategies. The formulation allows for large displacements and rotations in 3-D space. In recent years, Li, Gao et al.[11] gave an analytical solution to the static equilibrium equation of the riser, and calculated the vertical and horizontal bending deformation of the riser during deep-water drilling. Chainarong et al. [12] used the finite element method to calculate the three-dimensional static performance of a marine riser with fluid flow in the tube. The static solution methods mainly include finite difference and finite element methods. Similar studies have been conducted in Yang et al. [13], Sparks [14], Bernitsas et al. [15]and Zhou et al. [16].

In addition to the static analysis, an assessment of the mechanical behavior of the riser system also requires consideration of the dynamic response due to environmental loading. Simmonds (1980) [17.] established a fourth-order partial differential equation for lateral motion of the riser. The finite difference method was used to solve the dynamic response for different cases, corresponding to changes in sea currents, waves, floater motion, variable tension, and top end constraints. Time domain techniques are well suited to modelling non-linearities in structural geometry, loading and material behavior.[9]. Gardner and Kotch(1976) [18] used a finite element analysis in connection with the Newmark-β method to provide a time domain technique for the analysis of vertical risers. Hashemi-Safai(1983) [19] has outlined a general three-dimensional method for analysis of rigid risers and which was implemented in the computer program (RISER). Patel et al.(1984) [20] presented a two-dimensional finite-element computational method for determining displacements and stresses for vertical marine risers. The development and verification of flexible riser analysis software has been described by Engseth et al. (1988). [10] also referred to above. In 2013, Zhou and Liu [21] took the lead in proposing and carrying out theoretical research on the mechanical behavior of risers based on a joint representation of the marine environment and drilling conditions. The mechanical behavior of a riser attached to the "Offshore Oil 981" platform was successfully analyzed. Based on the analysis, it was found that the drill pipe inside the riser had a certain reduction effect on the lateral displacement of the riser. However, the drill pipe also experienced local collisions with the riser, which implied that wear and friction damage were found to require further studies. Similar research work has been reported e.g. by Trim [22], Sexton and Agbezuge [23], Malahy [24], Moe and Larsen[25], Ertas and Kozik[26].

Generally, the riser is regarded as a single pipe when dynamic analysis of risers in deep water is to be performed. However, during drilling operations, the drill string is rotating inside the riser, thus forming a pipe-in-pipe structure. Fig. 1(a) shows the sketch of the riser system corresponding to this representation. Several researchers have performed analysis by a pipe-in-pipe model: Harrison and Helle [27] provide an explanatory note on the interaction between the different components of pipe-in-pipe riser systems in connection with TLP/Spar dry tree risers and freestanding single line hybrid risers. The study was based on application of pipe-in-pipe (PIP) elements within a finite element program allowing to represent the dynamic interaction between the riser components. In 2009, Luk, et al.[28] used the ABAQUS finite element program to analyze the pipe-in-pipe model of a top tensioned riser system (TTR) attached to a Spar platform.. It was concluded the PIP guide spring model can be used for riser design in lieu of the PIP guide surface model. Blevins[29] conducted laboratory tests for a riser with drilling-induced vibrations, which revealed that fluid dynamic coupling can cause vibration of a riser with a rotating drill pipe and a water-filled annulus.

In most studies, the drilling riser is assumed to be a single pipe. Furthermore, most of the research on the effect of applying pipe-in-pipe models was performed in relation to risers with buoyancy cans in connection with SPAR platforms. There are few studies that are concerned with pipe-in-pipe models associated with drilling risers

also including the internal string. In this work, the mechanical response of a drilling riser system by application of pipe-in-pipe model has been investigated by the Riflex finite element program [30] which applies a penalty spring formulation in order to describe the contact.

The paper is organized as following. In Section 2, the single pipe and the pipe-in-pipe models are presented including both mechanical and environmental parameters. In Section 3, the basic static and dynamic analysis results are presented including a discussion of the differences found in deformation and stress characteristics for the two models. In Section 4, a drill string influence coefficient is proposed and discussed in connection with different loading conditions. Section 5 draws some important conclusions and outlines further work.

2. Modelling

2.1 Basics of Modelling

RIFLEX was developed as a tool for analysis of flexible marine riser systems, but it is also well suited for different types of slender structure, such as mooring lines, umbilical cables, and also for steel pipelines and conventional risers. This computer program is based on a nonlinear finite element formulation and is presently applied in order to simulate the physical behavior of the riser system.

The primary objective of the study was to analyze the effect from drill string/riser interaction on the riser system global response. In order to facilitate this within a reasonable computation time, the riser was first simplified as a single tube with constant diameter and thickness by applying a model that was truncated below the mudline. Interaction between the pipe and the oil was modelled by a lateral nonlinear spring. The top of the riser was connected to the vessel where the tensioner system was represented by application of a constant tension. The drilling platform can move around an initial offset, so a flex joint with a certain rotation stiffness was applied at the upper end of the riser. The lower end of riser is connected to wellhead, so a flex was also included at that location.

Although many control lines are installed at the outside of the riser, the stiffness and size of these are relatively small and were therefore ignored in the model. Similarly, the drill string was also simplified as a uniform elongated tube.

The force diagram of the riser determined by the above analysis is shown in Fig. 1(b). Both a pipe-in-pipe model and an equivalent single-pipe model were established to perform a comparison of results obtained by the two different modelling approaches.

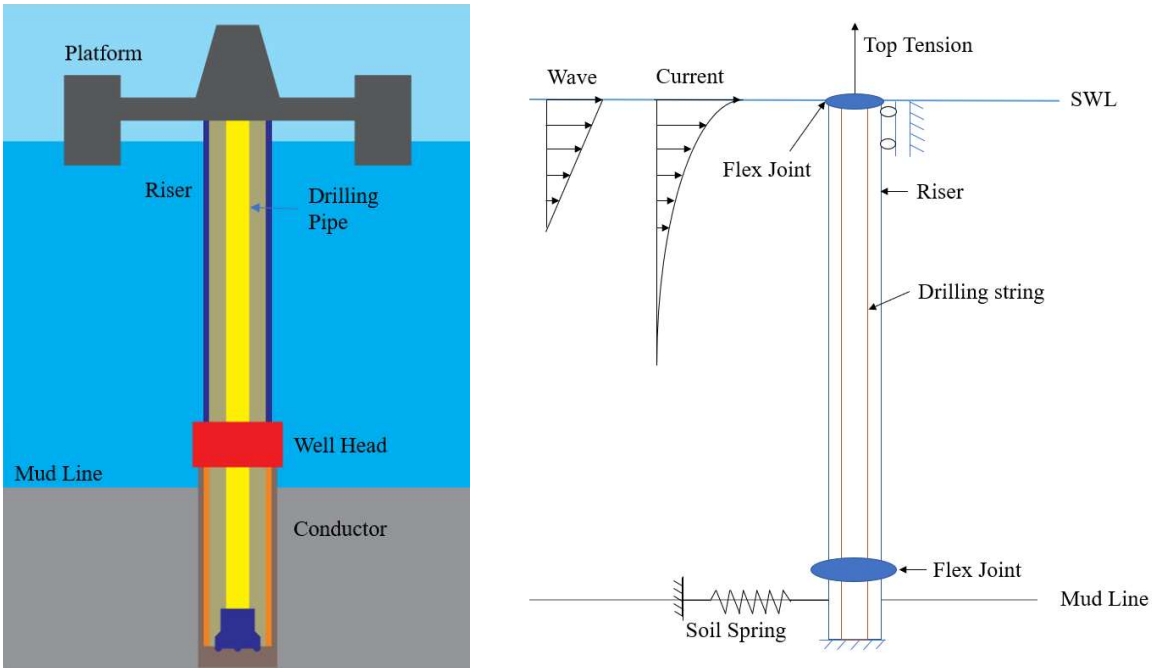

(a) (b)

Fig.1. Schematic layout and simplified force analysis model for a riser system during drilling operations

2.2 Equivalent Single Pipe Model

To analyze the difference in mechanical response between the PIP model and the traditional single-pipe model, a number of factors need to be fixed in order to ensure that the environmental loading and the resulting stress distribution are consistent. Therefore, an equivalent single-pipe model has been established based on the riser, drill string characteristics, top tension and other parameters used in actual drilling operations in the South China Sea. The following three steps were carried out in order to perform this analysis:

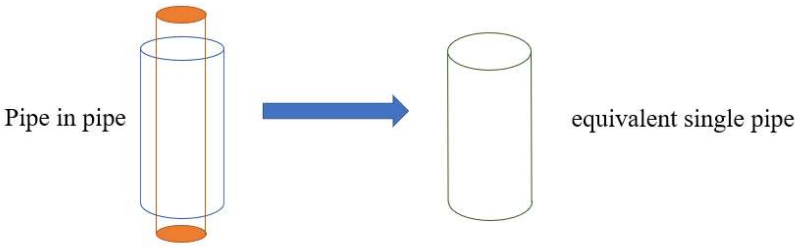

Fig.2 Transformation of PIP model into equivalent single pipe model

Step1 Set the values of mass, thickness and stiffness

In order to get the same mass and force distribution, the mass per meter of the equivalent single pipe model was set to be the sum of those for the drill string and the riser that were applied in the PIP model. The cross-section area of the equivalent single pipe was set to be the sum of the area of the drill sting and riser, which ensured that the single pipe and the PIP models had the same pipe weight and axial stiffness. Since both models are exposed to the same current load, the outer diameter of the equivalent single pipe model was set to be the riser outer diameter. The inner diameter of the equivalent single pipe model can be expressed as:

$$D_{i-equiv} = \sqrt{D_i^2 - d_o^2 + d_i^2} \tag{1}$$

where $D_{i-equiv}$ is the inner diameter of the equivalent single pipe; D_i is the inner diameter of the riser; d_o is the outer diameter of the drilling string and d_i is the outer diameter of the drilling string.

When creating an equivalent single pipe model for a pipe-in-pipe system, the stiffness of the two separate pipes were combined. This approach will be reasonable when assuming that the pipes are moving together uniformly when subjected to external and internal loading. The global motion of the equivalent model should therefore be close to the one for a real pipe-in-pipe system.

The combined stiffnesses (axial and bending, respectively) for two pipe systems can be written as:

$$EA = EA_1 + EA_2 \tag{2}$$

$$EI = EI_1 + EI_2 \tag{3}$$

where A is the equivalent area; I is the equivalent moment of inertia and E is the Young's modulus. The subscripts 1 & 2 represent the outer and inner pipe, respectively. E equals to 210000000kN/m^2.

The rotation stiffness values of upper and lower flex joints were set according to relevant drilling practice.[20]

The characteristic parameters associated with mass, diameters and stiffness properties are listed in Table 1.

Table 1

Mass, diameters and stiffness data of PIP model and equivalent single pipe model

Parameters	Outer riser	Inner drilling string	equivalent single pipe
Mass coefficient（kg/m）	313	28	341
Length(m)	1000	1000	1000
Outer diameter(m)	0.533	0.127	0.533
Inner diameter(m)	0.483	0.108	0.4782
Axial stiffness(N)	$8.3786*10^9$	$7.364286*10^8$	$9.115*10^9$
Bending stiffness(N*m^2)	$2.70933*10^8$	$1.34*10^6$	$2.72273*10^8$
Torsion stiffness(N*m^2/rad)	$3.522129*10^8$	$1.742*10^6$	$3.522129*10^8$
Upper flex joint rotation stiffness(Nm/deg)	$1*10^6$	-	$1*10^6$
Lower flex joint rotation stiffness(Nm/deg)	$6.3*10^7$	-	$6.3*10^7$

Step2 Water depth and top tension setting

In this paper, the water depth was set as 1000m, which is a representative average water depth for most wells in the South China Sea. The current and wave parameters for the target area are shown in Table 2. For the studies performed here, regular wave analyses were carried out where the base case wave height was set to 7.6m with a period of 9.6s. The characteristics of the current profile are provided in Table 3. Fig.3 shows the modelled configuration.

Table 2

Wave and current parameters for an area in the South China Sea

Parameter	Unit	Recurrence period (year)				
		1	10	25	50	100
Effective wave Hs	m	4.9	7.6	9.2	10.4	11.7
Max wave Hm	m	8.4	13.0	15.8	18.0	20.1
Effective period Ts	s	7.9	9.6	10.6	11.4	12.2
Max period Tm	s	8.3	10.2	11.2	12.0	12.9
Peak period Tp	s	9.3	11.3	12.5	13.4	14.3
Surface velocity		117	159	183	201	219
Velocity at 40m below	cm/s	109	139	152	161	169
Velocity at 80m below		80	105	112	116	120

Table 3

Current profile

Depth	Direction	Velocity
0	0°	1.59m/s
-30m	0°	1.39 m/s
-170m	0°	0.9 m/s
-200m	0°	0.8 m/s
-300m	0°	0.6 m/s
-500m	0°	0.3 m/s
-1000m	0°	0 m/s

Note: The depth at the sea surface is 0m, and negative values correspond to distances below the water surface.

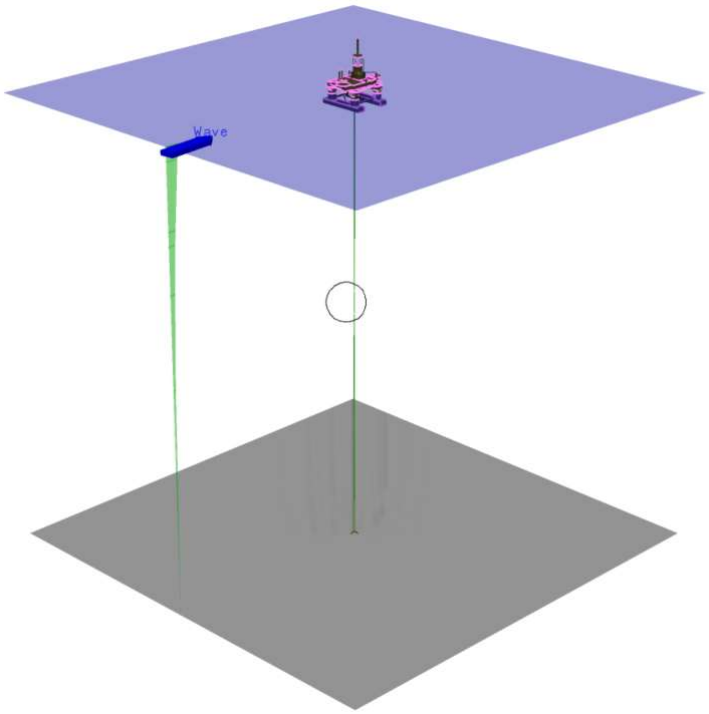

Fig.3 The system model as represented in the RIFLEX software

The submerged weights of the riser and the drill pipe were calculated as:

$$G_r^* = 6\times10^6 N \tag{4}$$

$$G_d^* = 2.18\times10^5 N \tag{5}$$

where G_r^* is the submerged weight of the riser in PIP model and G_d^* is the submerged weight of the drill string in the PIP model.

In this paper, the top tension was set to $1G^*$*(submerged weight of system)*, which means the top tension was equal to the total submerged weight of the pipes. In order to get the same force distribution, the top tension of the equivalent single pipe was set to:

$$T_s = T_r + T_d = 1\times\left(G_r^* + G_d^*\right) = 6.218\times10^6 N \tag{6}$$

where T_s is the top tension in the single pipe model, T_r is the top tension of the riser for the PIP model and T_d is the top tension of the drill string for the same model.

Step3 Setting the fluid density and global spring properties

The drilling fluid flow in the PIP model was simplified as shown in Fig. 4. The drilling fluid flows from the top to the bottom through the drill pipe and flows from the bottom to the top in the annulus between the drill pipe and the riser. The drilling fluid of the equivalent single pipe model was assumed to fill the entire annulus over the full length. According to deep-water well drilling experience, the density of the injected mud was set to 1.7g/cm3, and the density of the returned mud was set to 1.8g/cm^3. In order to directly compare the mechanical

responses between the two models, the corresponding effective tension distributions need to be the same. Therefore, the mud density of the equivalent single-tube model was calculated to be 1.68g/cm3.

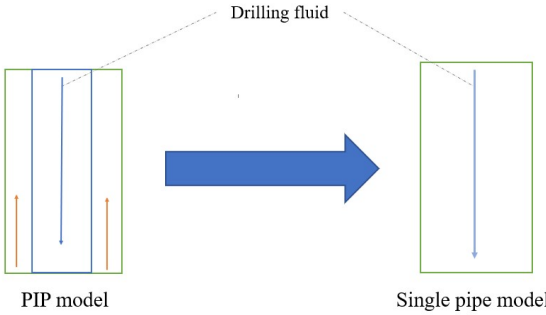

Fig.4 Schematic diagram of the simplified drilling fluid

The foundation reaction force was simplified and simulated using a nonlinear spring which was applied at the mud line. Based on the soil characteristics of the South China Sea and the drilling experience from multiple wells, the Force-Displacement relationship was set as shown in Table.4 below.

Table4

Force-displacement relations as basis for estimation of spring properties

Force	Displacement
0N	0m
1.379e5N	0.479m
2.206e5N	0.0783m
3.308e5N	0.123m
4.815e5N	0.208m

3. Results

3.1 Statistic analysis results

Since the top tension setting of the riser will have an impact on its static behavior, this paper considers top tension levels of 1.0G*(i.e. equal to the total wet weight of the pipes) and 1.2G* as the basis for the response analyses.

When the tension ratio was set to 1, the static analysis results of the equivalent single pipe model and the PIP model are as shown in Fig.5. For the displacement (Fig.5(a)), the response corresponding to the PIP model is the largest, with a maximum value that appears at a cross-section located 357m below the sea surface, and the lateral displacement has a value of 3.78m. This lateral displacement occurs at a cross-section which is located 0.18m away from the cross-section with the maximum value for the drill string (which is just the annular distance between the drill string and the riser). The displacement for the single pipe model is smaller than that for the PIP model. A likely reason is that the top tension of the single pipe model is larger than that of the PIP-riser, while the outer diameters and external loads for the two models are the same. For the effective tension distribution (Fig.5(b)), the calculation results for the two models are both smoothly decreasing from the top towards the bottom, and the effective tension near the bottom of the riser decreases sharply due to the heavy BOP and LMRP. For the bending moment and curvature (Fig.6(c-d)), the result shows that the largest bending moments occur near the top of riser in both models (disregarding the bending moment below the BOP). The difference between the bending moment and curvature for the PIP versus the single pipe model is generally small. However, slightly

larger values are observed seen for the PIP riser model.

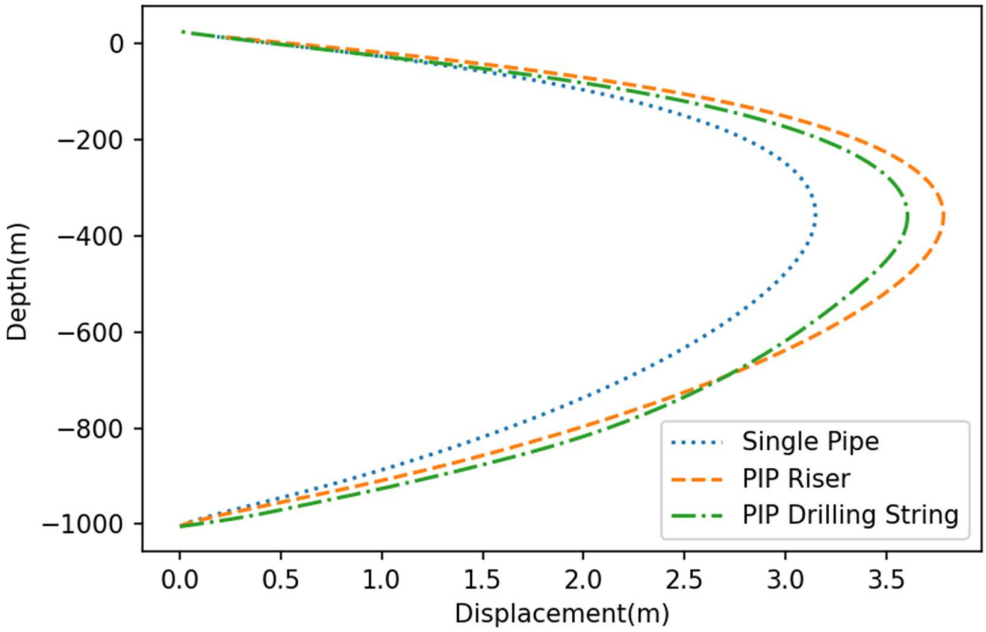

(a)

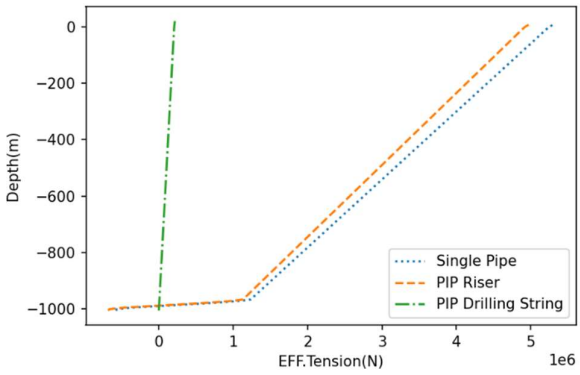

(b)

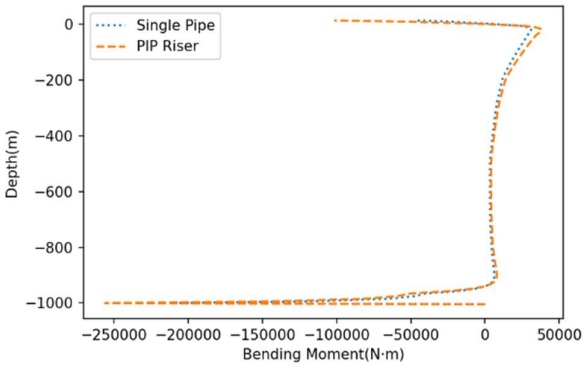

(c)

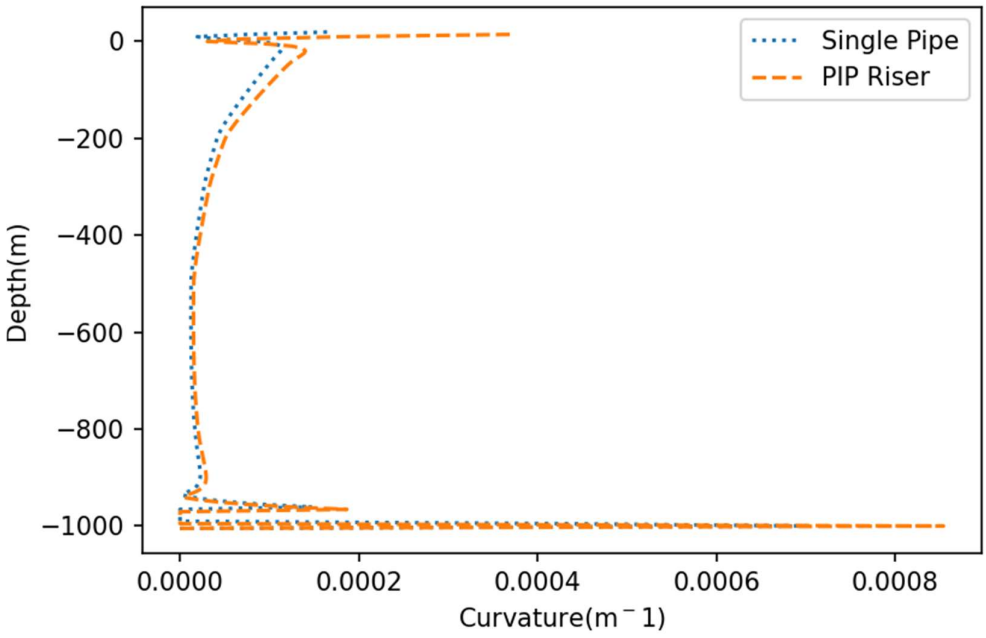

(d)

Fig. 5. Static analysis results for the case with top tension equal to 1G*

Fig. 6 shows the static analysis results for the equivalent single pipe model versus the PIP model when the tension ratio was set as 1.2. The variation of the tension distribution, lateral displacement and riser bending is similar to the calculated results for the tension ratio of 1. However, for the riser displacement (Fig.6(a)), the maximum value appears at 331m below the surface, and the lateral displacement value is 2.84m, which is smaller than the max displacement in Fig.5(a). Accordingly, it can be seen that the tension at the top of the riser has a significant effect on the lateral displacement as could be expected. The greater the tension, the smaller the lateral displacement. This is caused by the increase in the tension force and the resulting increase of lateral stiffness for the riser. Therefore, in actual operation, in order to prevent excessive lateral displacement of the riser, the tensioning force can be appropriately increased. If the tension is too large, the natural frequency of the riser will increase, which may be detrimental to the fatigue resistance of the riser [31]. For the bending moment and curvature (Fig.6(c-d)), the distributions are similar to those in Fig.5(c-d), while the maximum values of the bending moment and curvature are smaller than for the 1G* top tension case.

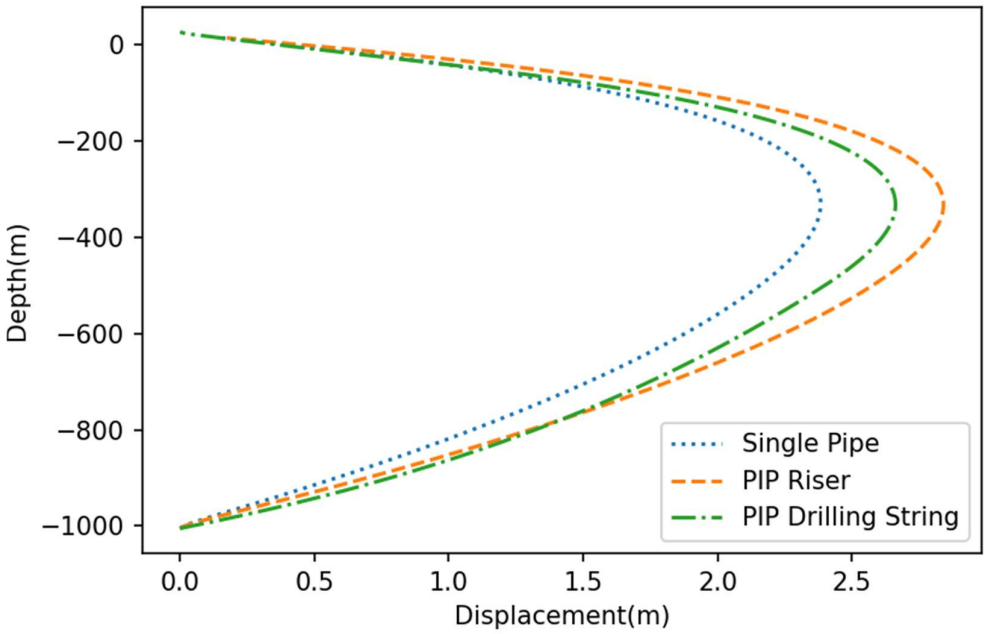
0
−200
−400
−600
−800
−1000
Depth(m)
0.0
0.5
1.0
1.5
2.0
2.5
Displacement(m)
Single Pipe
PIP Riser
PIP Drilling String

(a)

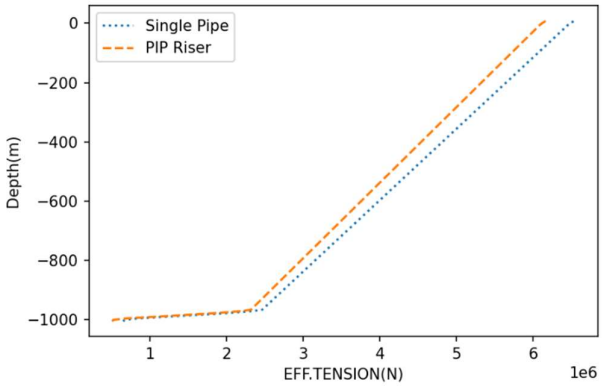
Single Pipe
PIP Riser
0
−200
−400
−600
−800
−1000
Depth(m)
1
2
3
4
5
6
1e6
EFF.TENSION(N)

(b)

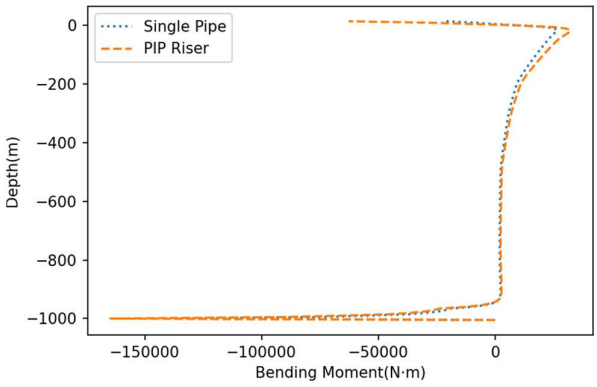
Single Pipe
PIP Riser
0
−200
−400
−600
−800
−1000
Depth(m)
−150000
−100000
−50000
0
Bending Moment(N·m)

(c)

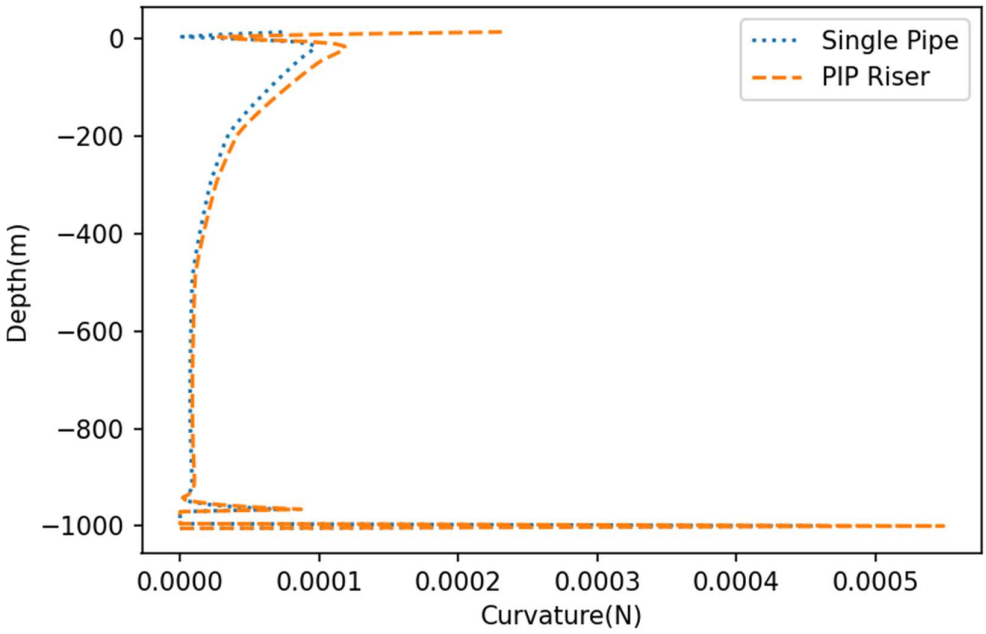

(d)

Fig. 6. Static analysis results for the case with top tension equal to 1.2G*

3.2 Dynamic analysis results

Fig.7 shows the results for the displacement, axial force, bending moment and curvature envelopes corresponding to the PIP model versus the single pipe model for the load case corresponding to 10 years return period (the wave height was7.6m and the wave period was 9.6s) and by applying a tension ratio of 1.2.

For the displacement envelope (Fig7(a)), the displacement of the PIP model reaches the maximum at 346m below the water surface, with a value of 4.6m. The maximum displacement of the single-pipe model also occurs at 346m below the water surface, with a maximum value of 3.96m. It can be seen that the displacement of the riser in the PIP model is larger than that of the single-pipe model.

For the axial force in the riser (Fig.7(b)), the two models both show little fluctuation based on the dynamic analysis. The general trend is that the axial force decreases from the top to the bottom of the riser, and the axial force near the bottom of the riser decreases sharply.

For the bending moment and the curvature of the riser (Fig.7(c-d)), since the two ends of the riser are equipped with flex joint with rotation stiffness in the model, the bending moment and curvature at both ends are the largest. Excluding the two ends of the riser, the bending moment and curvature diagrams each have two maximum points. The first extreme point is about 20 m away from the top of the riser and the second is about 120 m away from the bottom. From an overall perspective, the differences between the bending moment and curvature distributions are quite modest. However, at the extreme points, the bending moments for the PIP model are somewhat larger than those for the single pipe model.

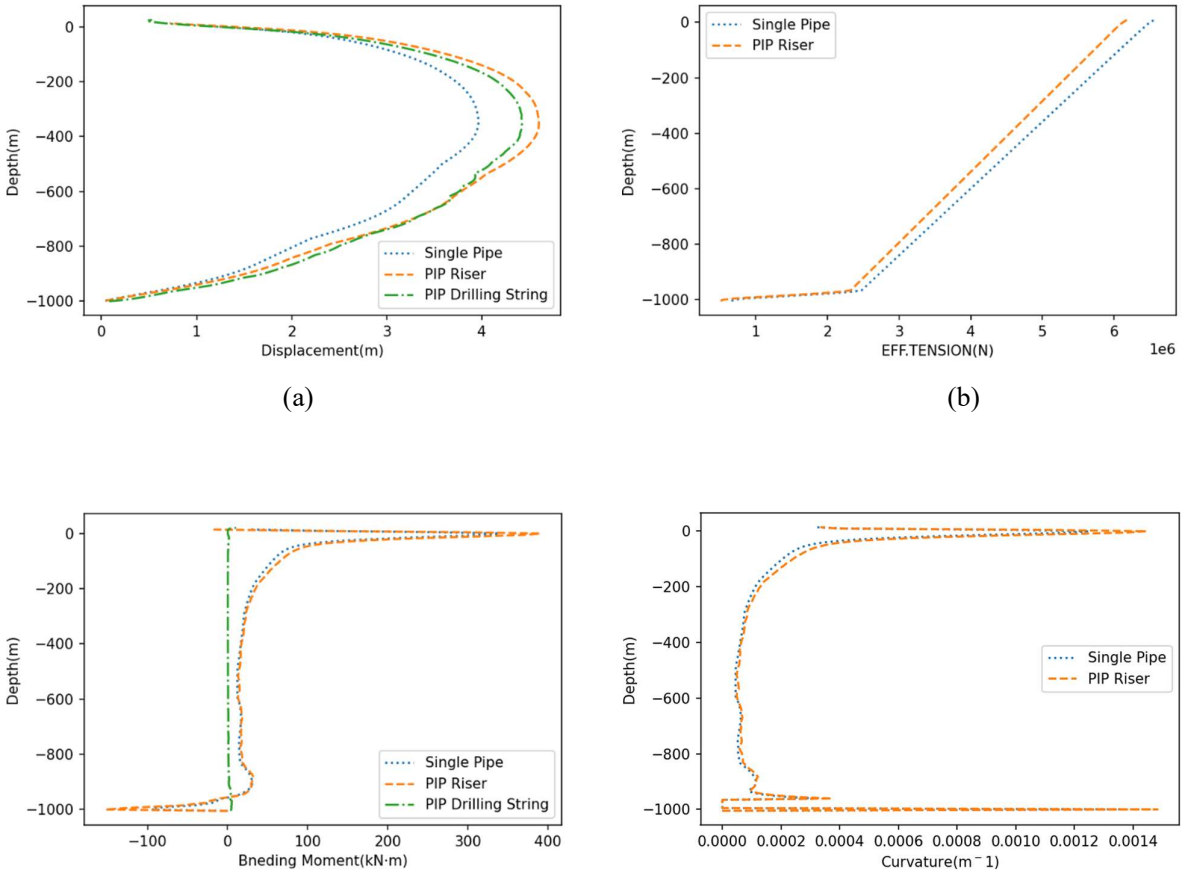

Fig.7. Dynamic analysis results (corresponding to wave amplitude = 7.6m, and wave period =9.6s)

Fig. 8 shows the displacement, axial force, bending moment and curvature diagrams for the PIP model and the single pipe model for environmental conditions with a recurrence period of 100 years (the wave height was set as 11.7m and the wave period was set as 12.2s). The surface velocity was set to 1.59m/s, and the top tension was equal to 1.2 times the wet weight of the pipes.

For the displacement diagram (Fig.8(a)), the displacement at the top of the riser increased to 2.96m, indicating that the worse the environment, the greater the drift of the platform at the surface. The maximum displacement of the riser for the PIP model (6.167m) is still greater than the maximum displacement of the riser for the single-pipe model (5.425m). The difference from the 10-year return period environment is that for the present environmental conditions, the maximum riser displacement of the two models appears at a position located 300m away from the top of the riser. In addition, the displacement diagrams for the riser and the drill string in the PIP model intersect in the range of 600-1000m below the water surface, which indicates that the riser and the drill string get in contact.

For the axial force envelope (Fig.8(b)), the general tendency is that the axial force decreases from the top to the bottom of the riser, and the axial force near the bottom of the riser decreases sharply going from a tensile force r to a compressive force. This shape of the diagram is similar to the result in Fig.7(b).

For the bending moment and curvature diagrams (Fig.8(c-d)), excluding the two ends of the riser, there are two critical cross-sections where the maximum values occur. The first extreme point is about 20 m away from

the top of riser and the second is about 45 m away from the bottom, which are the same locations as in Fig.7(c). However, the difference between the values at two extreme points for the PIP model versus the single pipe model is less than for the previous environmental condition.

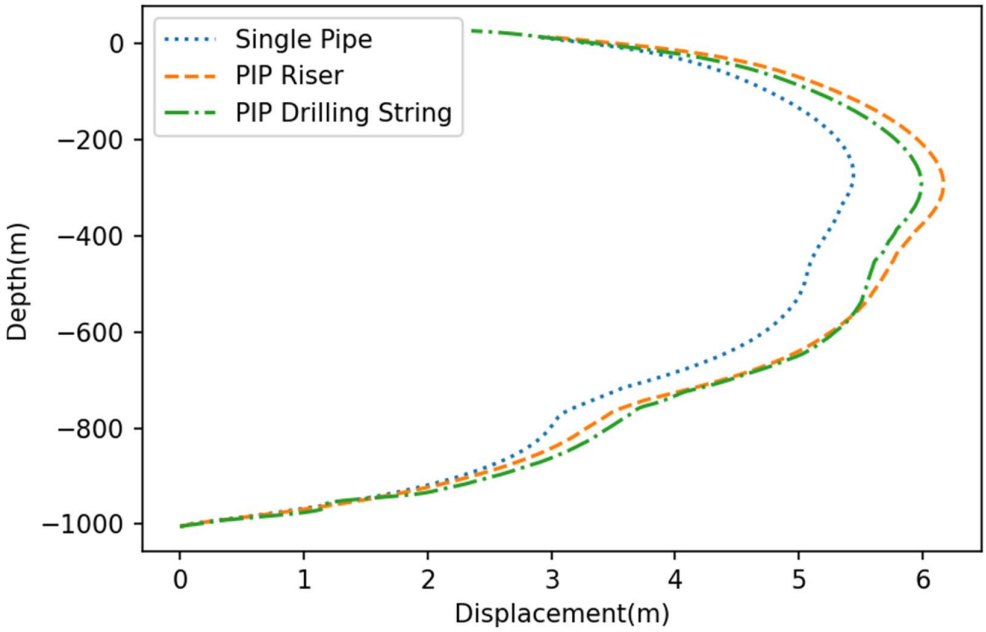

(a)

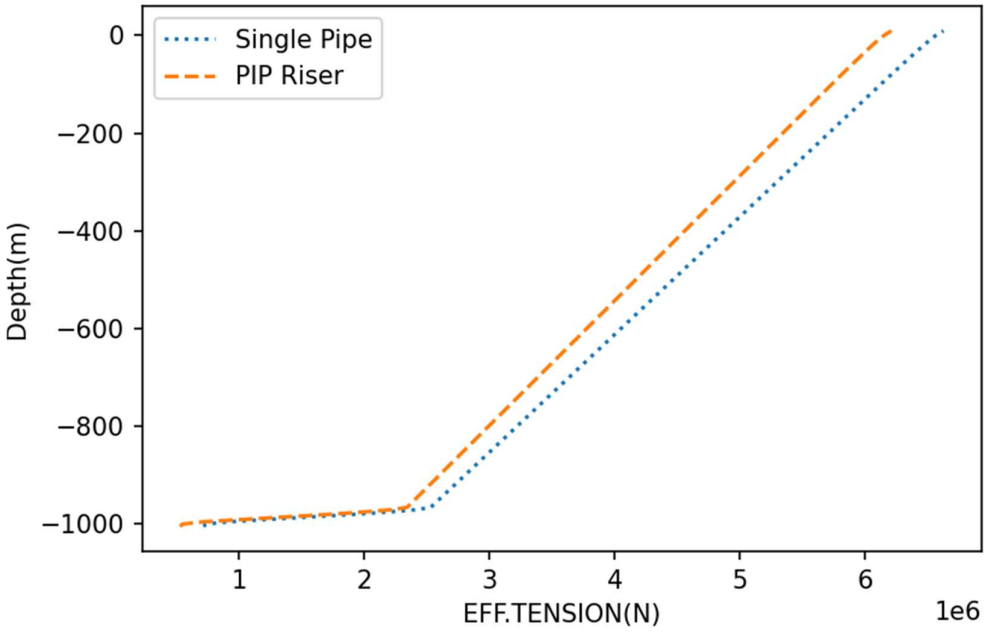

(b)

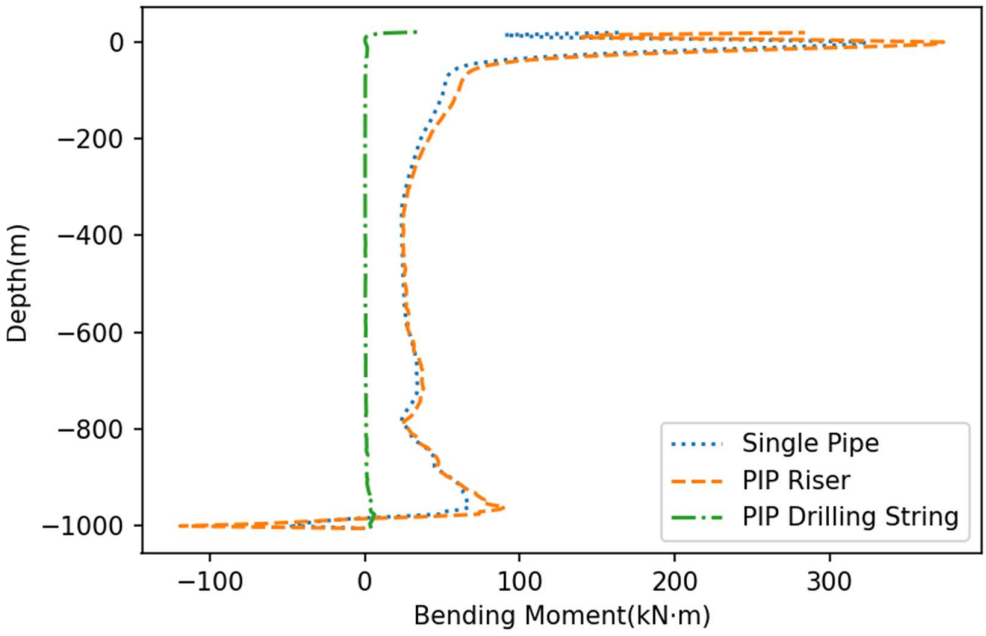

(c)

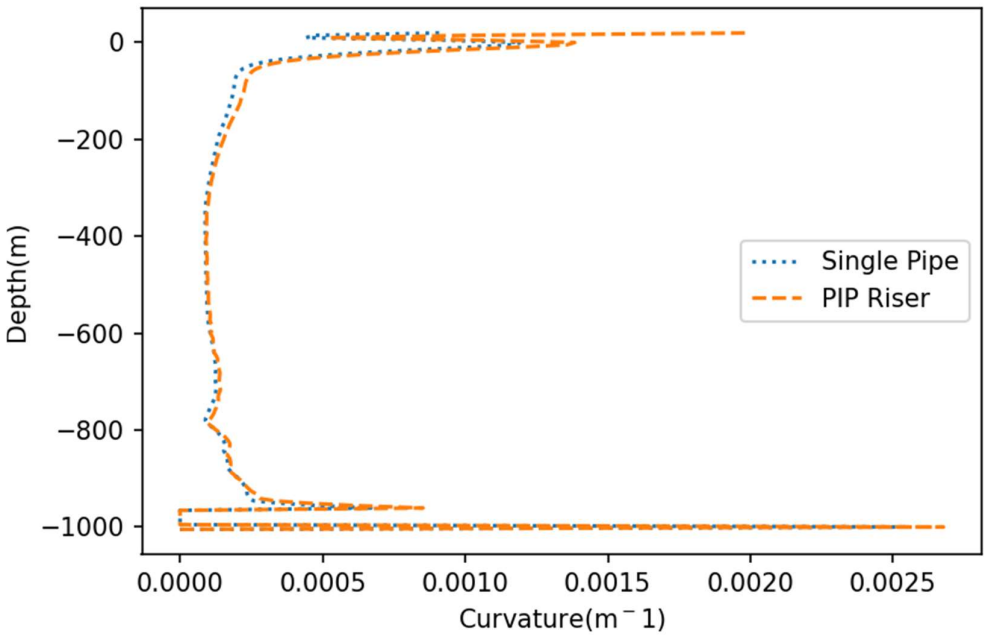

(d)

Fig.8. The dynamic analysis results (corresponding to a e wave amplitude = 11.7m, and wave period =12.2s)

Next, the variation of the displacement with respect to time was studied. Fig.9 illustrates this variation at the cross-section with maximum displacement (296.2m below the sea surface), when subjected to ocean currents.

It can be seen from this figure that the riser displacement for the PIP model is larger than that for the single-pipe model. The distance between the PIP Riser curve and the PIP drill string curve is sometimes equal to 0.18m, which indicates that the drill string and the riser are in contact with each other.

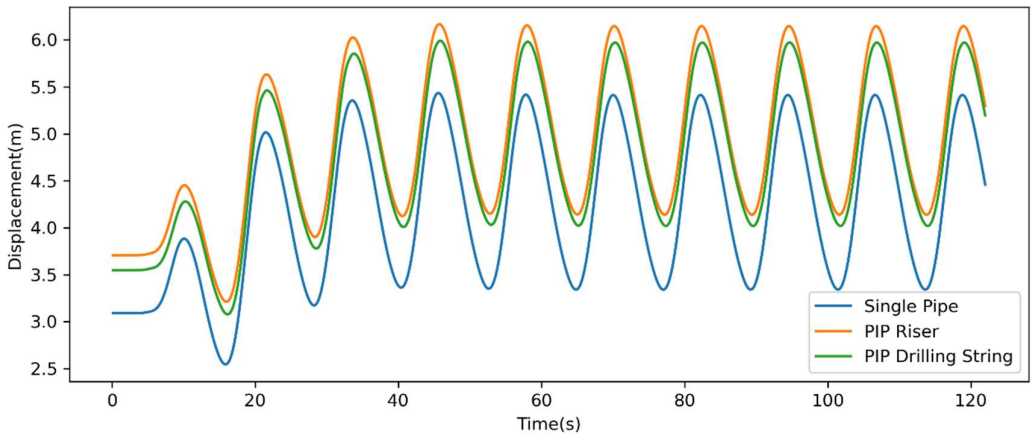

Fig.9. Time history of displacement at the cross-section with maximum lateral displacement.

Figure10 shows the variation with time for the bending moment at the two extreme cross-sections (20m below the top of the riser and 45m away from the bottom). For the cross-section located at 20m below the top of the riser (Fig.10(a)), it can be seen from the figure that the riser bending moment for the PIP model is larger than that for the single-pipe model. The time when the two curves reach the first peak is similar, which indicates that the two models behave similarly. As for the point 45m away from the bottom (Fig.10(b)), the peak of the PIP riser's bending moment curve and the maximum value of the single pipe's bending moment are very close. Compared with the single pipe model, the curve for the PIP model fluctuates at every peak. A possible reason is that the riser gets into contact with the drill string, which causes the bending moment to fluctuate.

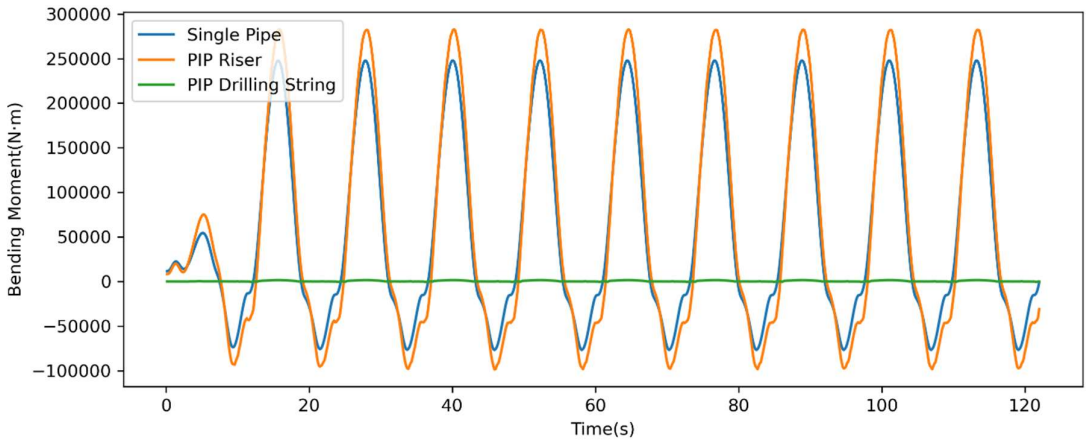

(a)-20m

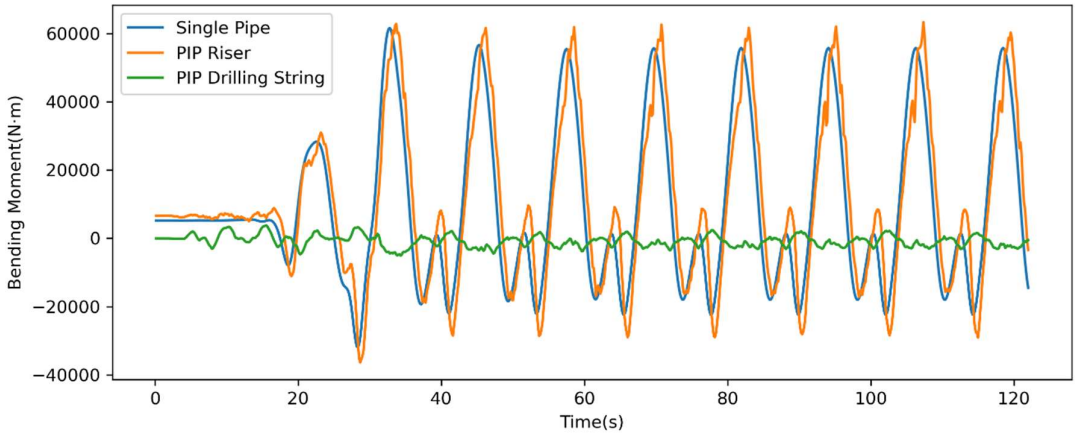

(b)-960m

Fig.10. Time history of bending moment for the critical cross-section.

4.Influence coefficient corresponding to different conditions

Based on the Multitube Moment Factor [32], a PIP influence coefficient has been proposed, in order to express the influence of the drill string on the mechanical behavior of the riser during the drilling process. The expression is as follows:

$$\beta(max)=\frac{\max(|Parameter_{PIP}|)}{\max(|Parameter_{equivalent}|)} \tag{6}$$

Here, β is the influence coefficient. $Parameter_{PIP}$ is the computed result for a specific response quantity (i.e. parameter) for the PIP model, while $Parameter_{equivalent}$ is the corresponding computed result for the equivalent single pipe model. The response quantity (i.e. parameter) can be the displacement, force, bending moment or curvature according to the focus of the analysis.

Based on the static analysis results corresponding to different top tension levels, the corresponding reference values of the displacement, bending moment and curvature for the two models were extracted. According to the data in Table 5, it is observed that the response for the PIP model is always lager than that for the single pipe model, which implies that the drill string inside the riser will influence the static analysis behavior of the riser in terms of displacement, bending moment and curvature. When the top tension increases, the displacement, bending moment and curvature of the riser in both models decrease. When the top tension is 1.2G*, the influence coefficient β is smaller than when the top tension is 1G*. However, the influence coefficients for the bending moment and curvature remain unchanged. These results show that appropriately increasing the top tension can reduce the influence of the drill string on the riser displacement, but the change in the top tension has no effect on the bending moment and curvature in the static analysis.

Table 5

The compared data of statistic analysis in two models

Top Tension	Model	Displacement	Bending Moment	Curvature
1G*	PIP Riser	3.785 m	37960 N·m	1.40e-4 m^{-1}
	Single Pipe	3.150 m	31110 N·m	1.13e-4 m^{-1}

	β	1.20	1.22	1.22
	PIP Riser	2.840 m	32130 N·m	1.186e-4 m^{-1}
1.2G*	Single Pipe	2.383 m	26430 N·m	9.71e-5 m^{-1}
	β	1.19	1.22	1.22

As for the dynamic analysis, the max displacement, bending moment and curvature at the critical cross-section has been extracted. As mentioned above, there are two such critical cross-sections with respect to maximum bending moments along the risers, which are at the upper and lower parts. According to Table 6, when the environmental conditions become more severe, the influence coefficient related to the riser displacement has decreased, while the influence coefficients for the bending moment and curvature in the lower riser section has increased. The main reason is due to alternating contact between the drill string and the riser in the lower part of the riser, causing the drill string to restrain the displacement of the riser in the case of harsh environmental conditions. The contact forces give rise to increased extreme bending moments, and accordingly the influence coefficient for the bending moment and curvature increases. The alternating contact between the two pipe strings will increase the fatigue damage for both the riser and the drill string.

Table 6

The compared data of dynamic analysis in two models

Wave Parameters	Model	Displacement	Bending Moment (-20m)	Curvature (-20m)	Bending Moment (-960m)	Curvature (-960m)
Hs=7.6m, Ts=9.6s	PIP Riser	4.599 m	390.50 kN·m	1.64e-3 m^{-1}	32.2 kN·m	3.30e-4 m^{-1}
	Single Pipe	3.940 m	339.36 kN·m	1.43e-3 m^{-1}	30.9 kN·m	3.17e-4 m^{-1}
	β	1.17	1.15	1.15	1.04	1.04
Hs=11.7m, Ts=12.2s	PIP Riser	6.167 m	373.62 kN·m	1.38e-3 m^{-1}	85.5 kN·m	8.52e-4 m^{-1}
	Single Pipe	5.425 m	324.36 kN·m	1.20e-3 m^{-1}	67.4 kN·m	6.69e-4 m^{-1}
	β	1.14	1.15	1.15	1.27	1.27

5.Conclusions

Considering the influence of a drill string being present within a riser, the objective of the present study was to quantify the difference between static and dynamic response for the two cases corresponding respectively to the PIP model and the single pipe model. The following conclusions are drawn based on the results that were obtained:

- For both static and dynamic analysis, the displacement of the riser obtained based on the PIP model is larger than for the single pipe model. The main reason is that the outer diameter and the external loads acting on the riser are the same for the two models. However, the single pipe model starts out with full effective tension, while for the PIP riser the effective tension effect from the drill string requires that contact between the two pipes is activated first.
- Although the bending moment and curvature of the PIP Riser in the static analysis are larger than for the

single pipe model, the differences between the PIP and the single pipe models are quite modest.

- An influence coefficient β which quantifies the effect of the drill string on the mechanical response behavior of the riser has been defined.
- When the top tension equals 1.2G*, the influence coefficient β for the displacement obtained from the static analysis is smaller than when the top tension is 1G*, while the influence coefficients for the bending moment and curvature remain unchanged for the two cases.
- Excluding the two ends of the riser, the bending moment and curvature diagrams of the riser have two maximum points. The overall shapes of the bending moment and the curvature diagrams between the two models are quite similar, but regarding the extreme values, the bending moment obtained based on the PIP model is larger than that for the single pipe model. This implies that the drill string has some influence on the resulting bending moments along the riser.
- For the most severe environmental loading, the riser and the drill string will give rise to significant impact events in the lower part of the riser for the PIP model.
- Contact between the drill string and riser will also implies that the riser displacement will be influenced, and hence the bending of the riser also tends to increase. This will increase the fatigue load for both the riser and the drill string.
- It is recommended as part of future research o study drill string and riser interaction for additional environmental conditions in order to map the variation of the values of the resulting influence coefficient in more detail.

Acknowledgments

The current study was carried out under the China Scholarship Council financial supports, at the Department of Marine Technology of the Norwegian University of Science and Technology. Special thanks to Engineer Wenxing Wang for his valuable technical support and consideration.

References

[1] Yang Jin, Cao Shijing. Current situation and developing trend of petroleum drilling technologies in deep water [J] .Oil Drilling & Production Technology, 2008 (02): 10-13.

[2] Yang, J., Liu, S. J., Zhou, J., Wang, P., Tang, H., Luo, J., Zhou, C. (2010, January 1). Research of Conductor Setting Depth Using Jetting in the Surface of Deepwater. Society of Petroleum Engineers. doi:10.2118/130523-MS

[3] Liu Caihong, Yang Jin, Cao Shijing, Cai Zhansheng. Drilling riser mechanical characteristics of marine deep water [J] .Oil Drilling & Production Technology, 2008 (02): 28-31.

[4] Liu Shujie, Xie Yuhong, Yang Jin, Xie Renjun, Zhang Chunyang, Lin Haichun, Peng Zuoru. Drilling riser dynamic characteristics of marine deep water [J] .Oil Drilling & Production Technology, 2009,31 (03): 1-4.

[5] William Fischer, Milton Ludwig. Design of floating vessel drilling riser[C]. SPE 1220, 1966.

[6] Ben G. Burke. An analysis of marine risers for deep water[C]. OTC 1771, 1973

[7] O'Brien P J, McNamara J F, Dunne F P E. Three-dimensional nonlinear motions of risers and offshore loading towers[J]. 1988:232-237.

[8] O'BRIEN P J, McNamara J F. Analysis of flexible riser systems subject to three-dimensional seastate loading[C]//BOSS'88. 1988: 1373-1388.

[9] Patel M H, Seyed F B. Review of flexible riser modelling and analysis techniques[J]. Engineering structures, 1995, 17(4): 293-304.

[10] Engseth A, Bech A, Larsen C M. Efficient method for analysis of flexible risers[C]//BOSS'88. 1988: 1357-1371.

[11] Li Yan, Wu Yanxin, Gao Deli. Analytic Solution of Flexural Deformation of Deep-water Drilling Riser [J] . Oil Field Equipment, 2011, 40 (7): 21-24.

[12] Chainarong Athisakul, Tinnakorn Monprapussorn, Somchai Chucheepsakul. A variational formulation for three-dimensional analysis of extensible marine riser transporting fluid[J]. Ocean Engineering, 2011, 38: 609-620.

[13] Jin Y, Wei M, Mengbiao Y A O, et al. Calculation method of riser top tension in deep water drilling[J]. Petroleum Exploration and Development, 2015, 42(1): 119-122.

[14] Sparks C P. Mechanical behavior of marine risers mode of influence of principal parameters[J]. 1980.

[15] Bernitsas M M, Kokarakis J E, Imron A. Large deformation three-dimensional static analysis of deep water marine risers[J]. Applied ocean research, 1985, 7(4): 178-187.

[16] Zhou S, Liu Q, Jiang W, et al. The discovery of “one third effect” for deep-water drilling riser: Based on the theoretical and experimental study of deformation characteristics of deep-water drilling riser by ocean currents[J]. China Offshore Oil and Gas, 2013, 25(6): 1-6.

[17] Simmonds D. G.. Dynamic analysis of the marine riser[C]. SPE 9735, 1980.

[18] Gardner T N, Kotch M A. Dynamic analysis of risers and caissons by the element method[C]//Offshore Technology Conference. Offshore Technology Conference, 1976.

[19] Safai V H. Nonlinear dynamic analysis of deep water risers[J]. Applied ocean research, 1983, 5(4): 215-225.

[20] Patel M H, Sarohia S, Ng K F. Finite-element analysis of the marine riser[J]. Engineering Structures, 1984, 6(3): 175-184.

[21] Zhou S, Liu Q, Jiang W, et al. The discovery of “one third effect” for deep-water drilling riser: Based on the theoretical and experimental study of deformation characteristics of deep-water drilling riser by ocean currents[J]. China Offshore Oil and Gas, 2013, 25(6): 1-6.

[22] Trim A D. Axial dynamics of deep water risers[C]//The First International Offshore and Polar Engineering Conference. International Society of Offshore and Polar Engineers, 1991.

[23] Sexton R M, Agbezuge L K. Random wave and vessel motion effects on drilling riser dynamics[C]//Offshore technology conference. Offshore Technology Conference, 1976.

[24] Malahy R C. A nonlinear finite element method for the analysis of offshore pipelines, risers and cable structures[C]//International offshore mechanics and arctic engineering. Symposium. 5. 1986: 471-478.

[25] Moe G, Larsen B Ø. Dynamics of deep water marine risers-asymptotic solutions[C]//The Seventh International Offshore and Polar Engineering Conference. International Society of Offshore and Polar Engineers, 1997.

[26] Ertas A, Kozik T J. Numerical solution techniques for dynamic analysis of marine riser[J]. J. Energy Resour. Technol.;(United States), 1987, 109(1).

[27] Harrison, R. I., & Helle, Y. (2007, January 1). Understanding the Response of Pipe-in-pipe Deepwater Riser Systems. International Society of Offshore and Polar Engineers.

[28] Luk, C. H., Yiu, F., and Rakshit, T. "Pipe-in-Pipe Substructure Modeling in Deepwater Riser Design Analysis." Proceedings of the ASME 2009 28th International Conference on Ocean, Offshore and Arctic Engineering. Volume 3: Pipeline and Riser Technology. Honolulu, Hawaii, USA. May 31–June 5, 2009. pp. 129-138. ASME. https://doi.org/10.1115/OMAE2009-79217

[29] Blevins R D, Coughran C S, Utt M E, et al. Drilling-induced riser vibration[C]//The 26th International Ocean and Polar Engineering Conference. International Society of Offshore and Polar Engineers, 2016.

[30] Fylling I, Larsen C M, Sødahl N, et al. Riflex user’s manual[J]. MARINTEK report, Trondheim, 1998.

[31] Huagui L. Dynamic analysis of offshore drilling riser[J]. 1993.

[32] Li Y. The Concept of Multitube Moment Factors in a Riser system and its Applications[C]//Offshore Technology Conference. Offshore Technology Conference, 1997.